



Zoological Journal of the Linnean Society, 2016, 177, 147–164. With 8 figures

## Synchrotron analysis of a ‘mummified’ salamander (Vertebrata: Caudata) from the Eocene of Quercy, France

JÉRÉMY TISSIER<sup>1</sup>, JEAN-CLAUDE RAGE<sup>1</sup>, RENAUD BOISTEL<sup>2</sup>,  
VINCENT FERNANDEZ<sup>3</sup>, NICOLAS POLLET<sup>4</sup>, GÉRALDINE GARCIA<sup>2</sup> and  
MICHEL LAURIN<sup>1\*</sup>

<sup>1</sup>Centre de Recherches sur la Paléobiodiversité et les Paléoenvironnements CR2P, UMR CNRS 7207, Sorbonne Universités, MNHN/CNRS/UPMC, Muséum national d’histoire naturelle, 57 rue Cuvier, CP 38 and 48, 75005, Paris, France

<sup>2</sup>IPHEP, Université de Poitiers UMR CNRS 7262, 6 rue Michel Brunet, 86073, Poitiers, France

<sup>3</sup>ESRF (European Synchrotron Radiation Facility), 71 avenue des Martyrs, 38000, Grenoble, France

<sup>4</sup>Evolution, Génomes, Comportement et Ecologie, CNRS, Université Paris-Sud, IRD, Université Paris-Saclay, 1 avenue de la Terrasse, F-91198, Gif-sur-Yvette, France

Received 21 May 2015; revised 5 August 2015; accepted for publication 18 August 2015

An incomplete ‘mummy’ from the Phosphorites du Quercy (presumed Eocene) was identified as a salamander during the 19<sup>th</sup> century. The specimen has now been computed tomography (CT) scanned, and this revealed the incomplete skeleton (with perfectly preserved bones) and soft tissues (lung). The fossil represents a new, well-characterized taxon. Despite the absence of the skull, several features allow a phylogenetic analysis. The fossil belongs to pseudosauvian caudates; it is tentatively assigned to the Salamandridae, although affinities with Plethodontidae cannot be definitely ruled out.

© 2015 The Linnean Society of London, *Zoological Journal of the Linnean Society*, 2016  
doi: 10.1111/zoj.12341

ADDITIONAL KEYWORDS: exceptional preservation – Lissamphibia – Phosphorites du Quercy – phylogeny – Salamandridae – skeleton – tomography – Urodela.

### INTRODUCTION

The ‘Phosphorites du Quercy’ (south-western France) encompass numerous fossiliferous localities, which are fissure fills in a karst. They have produced a large number of fossil vertebrates (Legendre *et al.*, 1997; Sigé & Pélissié, 2006), including a great diversity of tetrapods (mostly mammals, but also lissamphibians, squamates, and birds) spanning a period of over 30 Myr, from the Early Eocene (MP8–9) to the Early Miocene (MN3) (Sigé *et al.*, 1991; Rage, 2006). Most of these fossils have been recovered during industrial collecting of phosphate-containing rocks in the late 19<sup>th</sup> and earliest 20<sup>th</sup> centuries. The provenance and precise geo-

logical age of fossils collected at that time are unknown; such data are known only for fossils recovered during more recent field trips, which were initiated in the late 1960s (Rage, 2006). Most of the fossils are disarticulated bones, but a few exceptional specimens were described by Filhol (1873, 1877) and Rochebrune (1884) as ‘mummies’. Obviously, these fossils are not genuine mummies, but there is no available name for such exceptional fossils. They were sometimes labelled ‘external casts’ (Sanchiz, 1998), but as the internal organs are preserved (Laloy *et al.*, 2013), they are not merely casts. Therefore, we retain the term ‘mummy’, keeping in mind that this name is not fully adequate. The external morphology of the mummified animals is well preserved. For example, the scales on snake mummies are easily discernable, as are the eyes of the anuran *Thaumastosaurus gezei* Rage & Roček, 2007. The internal anatomy of the

\*Corresponding author.  
E-mail: laurin@mnhn.fr

mummy of *T. gezei* was recently revealed by X-ray tomography (Laloy *et al.*, 2013).

The mummified specimen studied here is registered under the number MNHN.F.QU17755 in the palaeontological collections of the Département Histoire de la Terre of the Muséum National d'Histoire Naturelle (MNHN, Paris, France). It was illustrated but not studied by Filhol (1877), who only identified it as a 'salamander' (Fig. 1). This specimen was perhaps previously described very briefly by Filhol (1873: 1557), who wrote: 'Finally, one last fossil specimen, from the same localities, must be identified as a large lizard. It includes the point of origin of the tail and the anchor of the posterior limbs that are folded anteriorly against the sides of the body' (our translation from the French original). This description perfectly fits the mummified specimen MNHN.F.QU17755, and our identification is reinforced by the fact that the only mummified squamates from the phosphorites in the MNHN collections and illustrated in the literature are portions of snake bodies. Yet, doubt persists because the size of the specimen (6 cm) does not fit that of a 'large lizard'. Nevertheless, the fact that the fossil was illustrated on the plate entitled 'Reptiles from the Phosphorites', not in the plate 'Batrachians from the Phosphorites', suggests that the specimen is the one described in 1873 as a 'lizard'. Filhol (1877) perhaps changed this identification in the legends. This fossil was not studied after the publication of Filhol's (1877) monograph. Even Estes (1981) did not cite it in his review of extinct salamanders.

Unfortunately, because no locality has been registered, specimens cannot be definitively placed in geological context and dated directly; however, here we present indirect evidence that suggests a Late Bartonian (MP16) to Late Priabonian (MP19 or 20) age.

Our specimen clearly belongs to a urodele (Lissamphibia: Caudata), a clade that includes salamanders and newts. Urodeles are generally regarded as the sister clade of Salientia (frogs and toads), and may have diverged from Salientia about 260–280 Mya, i.e. in the mid-Permian (Marjanović & Laurin, 2007). The fossil record is rather poor, with less than a hundred possible extinct species that mostly date from the Palaeogene and Neogene (Marjanović & Laurin, 2014). Their oldest known representatives were reported from the Bathonian (Middle Jurassic): *Marmorerpeton* from Great Britain (Evans, Milner & Mussett, 1988), *Urupia* from western Siberia (Skutschas, 2013), *Kokartus* from Kyrgyzstan (Skutschas & Martin, 2011), and probably an indeterminate form from Africa (Haddoumi *et al.*, 2015). This clade encompasses 691 currently recognized extant species (Frost, 2014), and they can be found in the holarctic and neotropical zones. The phylogeny of the group has been extensively studied, based on morphology (Gao & Shubin, 2001, 2012; Wang &

Evans, 2006; Zhang *et al.*, 2009) and on molecular sequences (Hay *et al.*, 1995; Wiens, 2007; Zhang & Wake, 2009), or on both (Larson & Dimmick, 1993; Wiens, Bonett & Chippindale, 2005; Frost *et al.*, 2006; Pyron, 2011; Pyron & Wiens, 2011). The monophyly of most high-level taxa has been demonstrated by recent studies (cited above). Below, we assess the affinities of the salamander mummy using a recently published data matrix to which we have added the new taxon.

## MATERIAL AND METHODS

### SPECIMENS

Aside from the fossil MNHN.F.QU17755 we used extant urodele specimens for comparisons. They have been selected to represent all extant urodele taxa typically ranked as families (Hynobiidae, Cryptobranchidae, Ambystomatidae, Amphiumidae, Plethodontidae, Salamandridae, Proteidae, Rhyacotritonidae, and Sirenidae). The inventory numbers of these specimens (when available) are shown in Table S1.

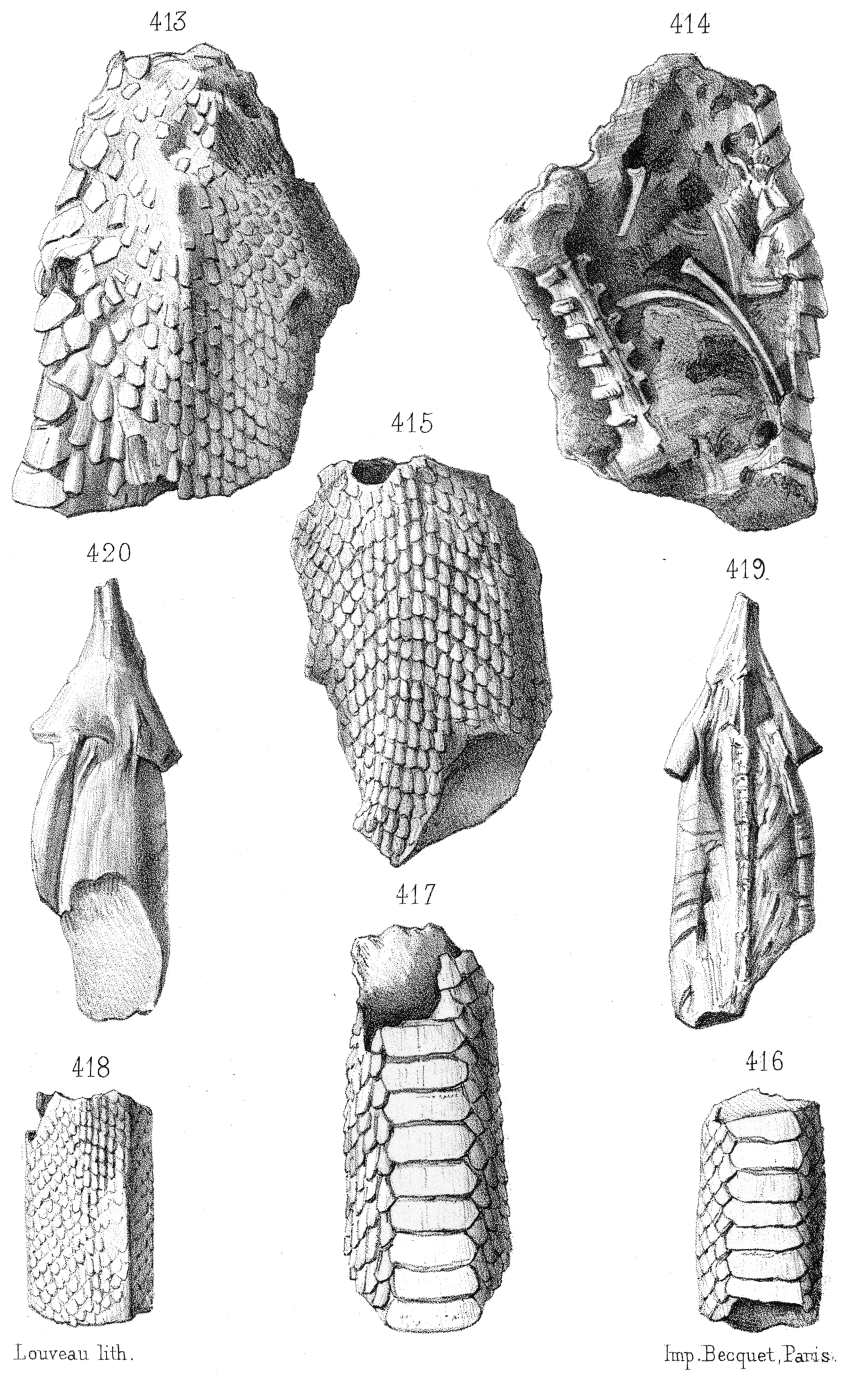
### TOMOGRAPHY

The fossil and recent material has been scanned by synchrotron (ID17 and ID19) or laboratory X-ray microtomography (depending on the specimen), to access the internal anatomy, and more particularly the postcranial skeleton. The list and acquisition parameters of the extant and extinct salamander images are summarized in Table S1.

The images of the mummy from the Phosphorites du Quercy have been obtained by propagation phase-contrast X-ray synchrotron microtomography using a high-energy filtered polychromatic beam at the ID19 beamline of the European Synchrotron Radiation Facility (ESRF, Grenoble, France; see Table S1 for parameters). For the tomographic reconstruction, a phase retrieval approach was used from a single long propagation distance using the Paganin filter of the PyHST2 algorithm (Paganin *et al.*, 2002; Mirone *et al.*, 2014). This technique has the benefit of detecting low levels of density, and thus gives better contrast between the mineral matrix of the fossil. The radiographic images (2048 × 2048 pixels) were acquired through a CCD FReLoN 2k camera.

### SEGMENTATION

Segmentation is a technique that consists of isolating and extracting, in three dimensions, elements of interest for study from tomography data. On the tomograms obtained for the mummy of the salamander, two types of elements have been extracted: bones (mostly) and soft tissues. This paper will present the data on bones and the lung.



Reptiles des Phosphorites.

**Figure 1.** Original drawings of the ‘mummified’ salamander in ventral (numbered 420) and dorsal (numbered 419) views, from Filhol (1877). In Filhol’s legend, drawing 419 would represent a portion of the snake *Coluber lafonti*, and only drawing 420 would represent the salamander. Note that the drawings are inverted (they are lithographs), and that the specimen is represented upside down (i.e. cranial direction down). The title of the plate is ‘Reptiles of the Phosphorites’ (translation by the authors).

AVIZO 6.3 (Visualization Sciences Group, Burlington, MA, USA) has been used for the segmentation and visualization of the data. Angles were measured (for descriptive purposes) with the ‘angle’ tool of the software. They are presented in the section ‘Description’.

#### PHYLOGENETIC ANALYSIS

To understand the systematic relationships between the fossil and the other urodeles, we performed phylogenetic analyses with a parsimony algorithm on morphological and molecular data using the heuristic search algorithm in PAUP\* 4.0 (Swofford, 2003). The matrix (available in NEXUS format in Appendix S1) is based on Wiens *et al.* (2005), which includes all major clades of urodeles, but it was partly recoded for the morphology of extant taxa, based on our scans, and data for the mummy was also added. It includes 326 morphological characters, 45 of which were scored for the mummy (vertebral skeleton, hindlimb, pelvic girdle, and lung), and 1742 molecular characters (212 for the ribosomal RNA and 1530 for RAG-1), not scored for the specimen. Characters that appear to form morphoclines were ordered following the suggestions of Wiens *et al.* (2005) because recent simulations have shown that this should improve phylogenetic accuracy (Grand *et al.*, 2013; Rineau *et al.*, 2015). Two characters were added and scored for all taxa: vertebral centrum (character 2069: 0, amphicoelous; 1, opisthocoelous) and lung (character 2070: 0, present; 1, absent).

A thousand random replicates and tree bisection and reconnection branch-swapping were employed. Multi-state taxa were interpreted as polymorphic and gaps were interpreted as missing data. Node support values were determined using non-parametric bootstrapping, with 100 replicates per analysis.

Two gymnophionans (*Dermophis* and *Ichthyophis*) are used as a compound outgroup, and two anurans (*Discoglossus* and *Ascaphus*) were included to better characterize the root of Urodela. The other taxa of the matrix were chosen by Wiens *et al.* (2005) to represent the major clades of urodeles.

#### SYSTEMATIC PALEONTOLOGY

CAUDATA FISCHER VON WALDHEIM, 1813

PSEUDOSAURIA BLAINVILLE, 1816

?TREPTOBRANCHIA FROST, GRANT, FAIVOVICH *ET AL.*,  
2006

?SALAMANDRIDAE GOLDFUSS, 1820

#### **PHOSPHOTRITON GEN. NOV.**

##### *Etymology*

Greek φωσφόρος, phosphorus, in reference to the nature of the sediment; triton, a frequent suffix in the genus names of salamanders.

##### *Diagnosis*

As for the type species and only known species.

#### *PHOSPHOTRITON SIGEI SP. NOV.*

##### *Holotype*

An incomplete ‘mummified’ body of a salamander (MNHN.F.QU17755).

##### *Type locality*

Unknown locality of the Phosphorites du Quercy, south-western France.

##### *Horizon*

Likely Eocene (late Middle or Late Eocene).

##### *Etymology*

After Bernard Sigé, one of the main contributors of the Quercy campaigns.

##### *Diagnosis*

A non-elongate, lunged caudate amphibian referred to Pseudosauria, based on the presence of a median process on the ischium, clearly separated para- and diapophyses on trunk vertebrae, spinal nerves exiting intravertebrally in caudal vertebrae, and in lacking articulated ribs in the caudal region. Tentatively referred to Salamandridae on the basis of having a paired sacral rib, a median notch in the posterior border of the neural arch, neural spines low on trunk vertebrae, neural spines present on caudal vertebrae, a bony lamina connecting para- and diapophyses, and spinal nerves exiting intravertebrally in posterior trunk vertebrae. Differs from other Pseudosauria by the presence of an anterior interzygapophyseal ridge, a dorsal alar process extending between the parapophysis and prezygapophysis and amphicoely of centrum, an association of characters that is unique within the clade.

##### *Description*

###### *External morphology*

The fossil (Fig. 2) shows body proportions that are fairly primitive for tetrapods, and that are retained among extant taxa in many urodeles and squamates. It is approximately 60 mm long, about 2 cm wide anteriorly, and its thickest part is slightly more than 1 cm. The head, anterior part of the thorax, and anterior limbs are lacking. The posterior limb and the tail are incomplete. The specimen is globally fusiform, except for the hindlimb fragments that emerge from the pelvic area and are directed anteriorly. The caudalmost part is much thinner (< 0.5 cm wide) than the anterior part. The specimen is best preserved on its left side.

The skin does not show any scales, which suggests that it is a salamander, rather than a squamate. In dorsal view (Fig. 2A), the vertebral column and some

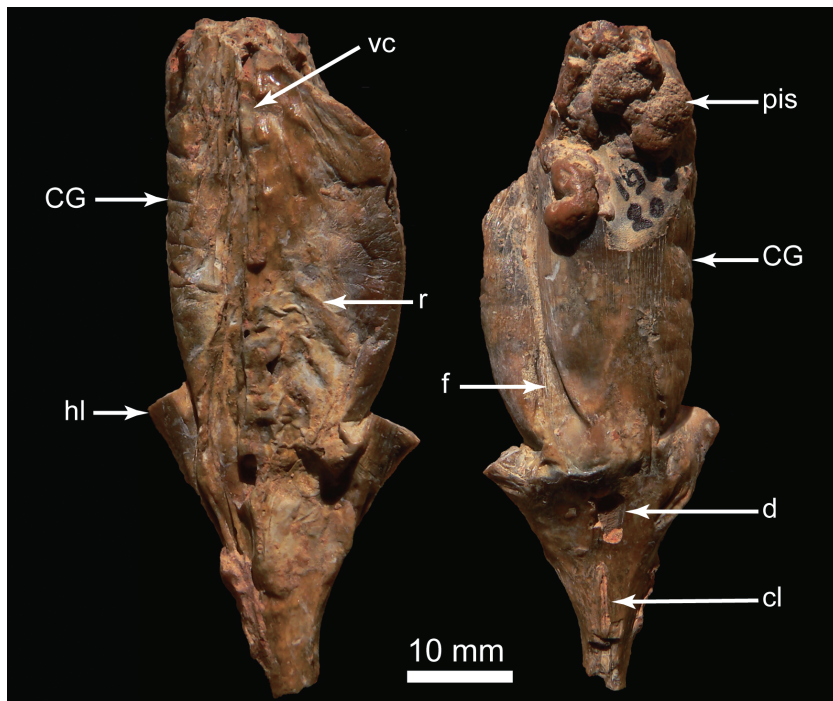


**Figure 2.** Photograph of MNHN.F.QU17755, holotype of *Phosphotriton sigei* gen. et sp. nov. in dorsal (A) and ventral (B) views. The old collection number (1903–20) is partially visible. CG, costal groove; cl, cloaca; d, damaged area; f, fold; hl, hindlimb; pis, pisolith; r, rib; vc, vertebral column.

ribs can be distinguished beneath the skin. At least five costal grooves appear on the left side of the mummy, in dorsal view. They are found on most caudates, with different counts according to the species. A longitudinal fold, going from the level of the pelvic girdle to the anterior part of the specimen, is visible on the ventral face (Fig. 2B), and may result from the position of the animal on the substratum during fossilization. A longitudinal slit of a few millimeters long, posterior to the hindlimbs, probably represents the cloaca. It is not to be confused with the small square damaged area just anterior to it, which is a missing fragment of skin. Cranially, pisoliths (mineral concretions) are visible where the inside of the thorax once was.

#### Skeleton

Tomography revealed that the whole skeleton of the actual part of the animal is preserved and is in anatomical position (Fig. 3A). Six trunk vertebrae (v3–v8) are complete, each being articulated to a complete rib on both sides of the specimen. Two other, more anterior vertebrae are incomplete, here labeled v1 and v2. Throughout this description, the position of vertebrae refers to the specimen in its current state, not as if it were complete, i.e. v1 is the anteriormost preserved vertebra, not the atlas. This is necessary because the number of missing vertebrae is uncertain. The first

preserved vertebra (v1) is connected to a complete rib on the left side, but the right side is missing. v2 is connected to a complete rib on the left and to an incomplete rib (the proximal end is not preserved) on the right. The left rib-bearer is incomplete. Two other rib fragments are also present anterior to v1, for which the proximal extremities are missing: they must have been connected to two other unpreserved vertebrae, anterior to v1. Seventeen trunk ribs are preserved (at least partially): ten on the left and seven on the right.

The sacrum (v9) is preserved and articulates to v8 anteriorly and to the first caudosacral vertebra (CS1). Rib-bearers are more massive than on the other vertebrae, and each articulates to a sacral rib. These ribs are shorter than trunk ribs, but stouter. v9 presumably articulated (through cartilaginous tissues) to the ilium, but the connection is not preserved (in fact, no cartilage is preserved at all in this specimen). The ilium articulates to the ischium, which connects to its mate ventrally. The pubis is not preserved. The femur is incomplete on both sides: it articulates to the ilium; its distal extremity is broken off.

Two caudosacral vertebrae and three caudals are preserved and complete to subcomplete. Shrunken rib-bearers are present but no ribs articulate with them. In addition, a fragment of a caudal vertebra (C4) is connected to the last caudal vertebra but it is very poorly preserved. Therefore, the specimen possessed at the

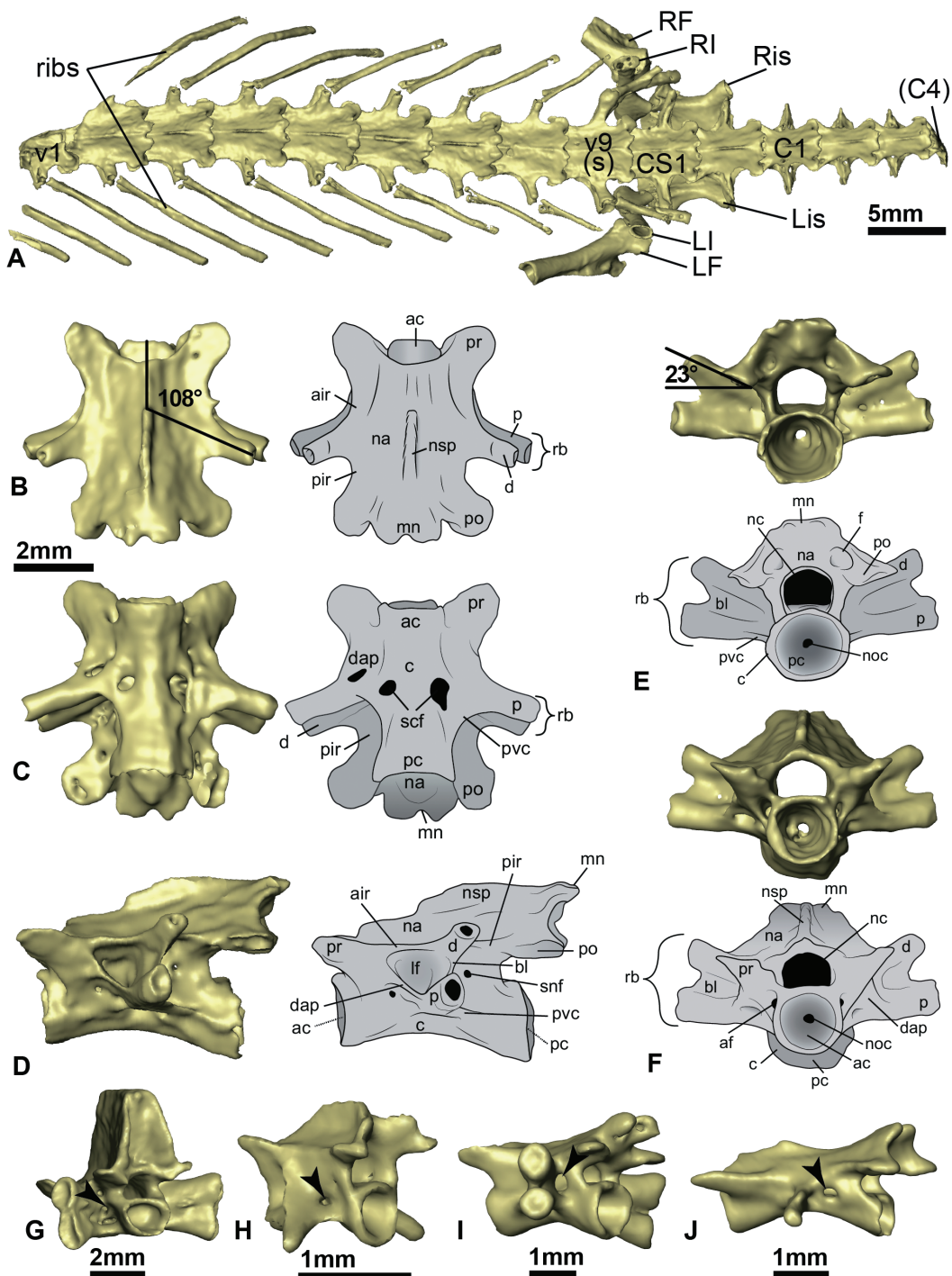


**Figure 3.** A, skeleton of MNHN.F.QU17755 in dorsal view. B–F, trunk vertebra (v6) in dorsal (B), ventral (C), left lateral (D), posterior (E), and anterior (F) views. G–J, trunk vertebrae in posterolateral view, illustrating a type-III disposition of the spinal nerves (Edwards, 1976) in *Paramesotriton deloustali* (Bourret, 1934) (G), *Pseudobranchus striatus* (LeConte, 1824) (H), *Ambystoma opacum* (Gravenhorst, 1807) (I), and *Bolitoglossa mexicana* Duméril, Bibron and Duméril, 1854 (J). Abbreviations: ac, anterior cotyle; af, anterior foramen; air, anterior interzygapophyseal ridge; bl, bony lamina; c, centrum; d, diapophysis; dap, dorsal alar process; f, fossa; If, lateral fossa; LF, left femur; LI, left ilium; Lis, left ischium; mn, median notch; na, neural arch; nc, neural canal; noc, notochordal canal; nsp, neural spine; p, parapophysis; pc, posterior cotyle; pir, posterior interzygapophyseal ridge; po, postzygapophysis; pr, prezygapophysis; pvc, posterior ventral crest; rb, rib-bearer; RF, right femur; RI, right ilium; Ris, right ischium; s, sacrum; scf, subcentral foramen; snf, spinal nerve foramen.

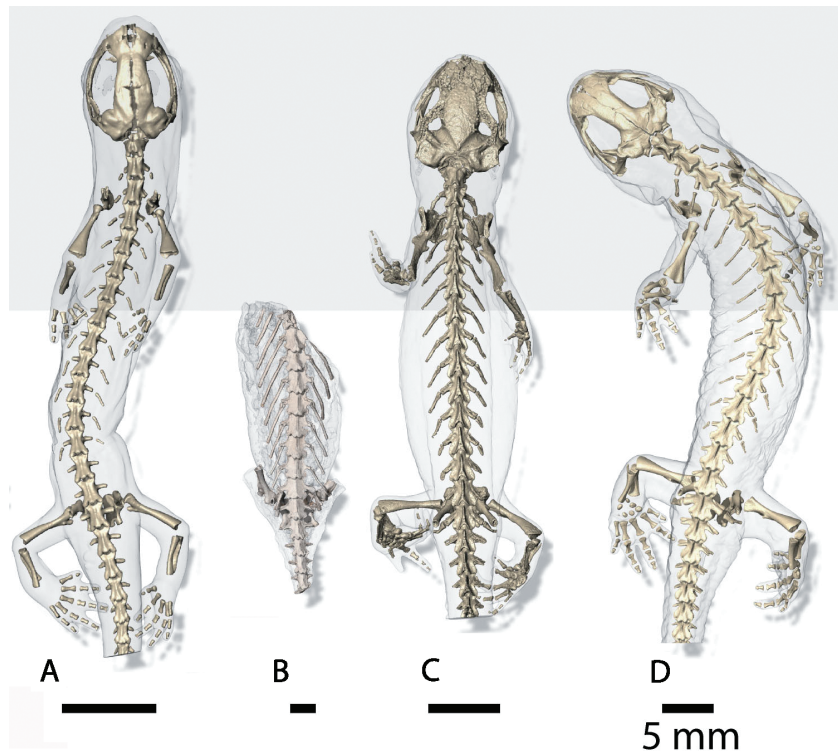


**Figure 4.** Three-dimensional reconstruction of the skeleton of *Phosphotriton sigei* gen. et sp. nov. (B), scaled to the same length as other Eurasian urodeles: a European plethodontid, *Hydromantes italicus* Dunn, 1923 (A), and two salamandrids, *Hypselotriton orientalis* (David, 1873) (C) and *Salamandra salamandra* (Linnaeus, 1758) (D).

very least 11 trunk vertebrae (sacrum included) and six caudal vertebrae, but obviously more because the tail and trunk region are very incompletely preserved (Fig. 4).

#### Vertebral column

The vertebrae display the overall morphology that occurs in short-bodied, four-limbed urodeles (Estes, 1981; Ratnikov & Litvinchuk, 2007; Fig. 3B–F). All vertebrae are amphicoelous. There are neither subcentral keels nor basapophyses. In ventral view (Fig. 3C), the centrum is hourglass-shaped. The shape, size, and number of subcentral foramina are highly variable along the vertebral column. A median notch indents the neural arch posteriorly, which therefore forms two posterior rounded projections (Fig. 3B and C); the posterior part of the neural spine is also affected by the notch. The neural canal is wide, high, and its cross section is pentagonal. Within the neural canal there are no visible spinal cord supports (Skutschas & Baleeva, 2012), but because these structures are very thin and difficult to see on tomograms (P.P. Skutschas, pers. comm., 2014) they cannot be definitely regarded as absent. Furthermore, a little prominence is in fact visible on some vertebrae, on the ventrolateral part of the neural canal, which could be interpreted as the base of such sup-

ports. The articular facets of the prezygapophyses and postzygapophyses are circular. The anterior borders of the prezygapophyses protrude beyond the anterior limit of the centrum (Fig. 3B). The posterior edges of the postzygapophyses extend beyond the posterior extremity of the centrum. In posterior view, the articular surfaces of the postzygapophyses make an angle of approximately 23° with the horizontal (Fig. 3E).

Each rib-bearer comprises a dorsal and a ventral process. These processes are here referred to as the diapophysis (dorsal) and parapophysis (ventral), following Skutschas (2013), although homology with the diapophyses and parapophyses of other tetrapods is not demonstrated (Wake & Lawson, 1973). The rib-bearers are directed posterolaterally: the angle between them and the vertebral axis (the ‘transverse process angle’ or ‘TPA’ in Babcock & Blais, 2001) is around 108° (Fig. 3B). The dia- and parapophysis are widely separated, and they are connected by a bony lamina that extends along most of their length (Fig. 3E and F). The diapophysis is slightly posterior to the parapophysis, and is more slender. The articular surfaces for ribs are circular.

The anterior and posterior interzygapophyseal ridges are well developed and horizontal (Fig. 3B and C). The weak posterior ventral crest forms a horizontal ridge

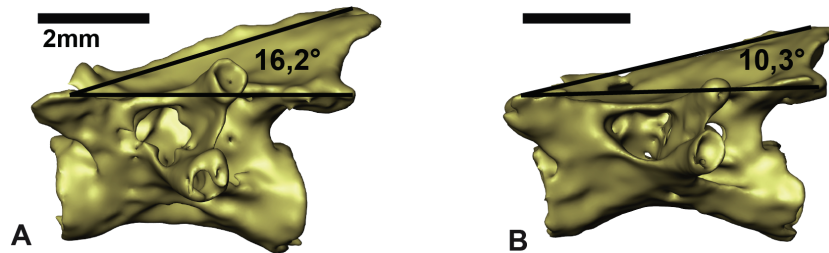


**Figure 5.** A, v1 in left lateral view with value for the angle between the posterior end of the neural arch and the zygapophyseal plane. B, v8 in left lateral view, with value of the same angle.

(Fig. 3C, D and E). The vertebrae lack an anterior ventral crest, but an oblique crest joins the parapophysis to the prezygapophysis. It is analogous (but perhaps not homologous) to the dorsal alar process (Gardner, 2003) that occurs in the Sirenidae; for the sake of convenience, we call this crest ‘dorsal alar process’, as that of sirenids (Fig. 3D and F). Between this dorsal alar process and the anterior interzygapophyseal ridge is a deep fossa (which we call the lateral fossa) in which opens a large foramen (Fig. 3D). Aside from sirenids, the dorsal alar process appears to exist only in pleurodeline salamandrids (Bailon, Rage & Stoetzel, 2011).

#### Trunk vertebrae

These vertebrae are very homogeneous in size and shape. The centrum measures approximately 5.7 mm long, and the vertebrae are between 6.4 (v8) and 6.0 (v3) mm wide (rib-bearers included); their width increases caudally.

The neural arch is moderately vaulted and its position is rather elevated with regard to the centrum: the angle formed between the posterodorsal end of that arch and the zygapophyseal plane is 16° for the anteriormost (Fig. 5A) and 10° for the posteriormost vertebrae (Fig. 5B). The anterior margin of the neural arch is concave between the two prezygapophyses (Fig. 3B). The neural arch bears a neural spine. The latter is thin and poorly developed, and it is strongly reduced on the posteriormost trunk vertebra (v8) (Fig. 3A). When present, it does not extend to the anterior extremity of the neural arch, but only halfway.

In anterior view (Fig. 3F), a large foramen (termed the anterior foramen here) is present on each side, laterodorsal to the anterior cotyle; it pierces the base of each prezygapophyseal buttress. It is connected to the subcentral foramen (where present; Fig. 3C). In posterior view, a paired fossa (Fig. 3E) is present on the posteroventral face of the posterior part of the neural arch, mediadorsal to the postzygapophyses. It is shallow and ellipsoid. A notochordal canal is present at the centre of the cotyles and is rather small (Fig. 3E and F).

The parapophysis is horizontal, whereas the diapophysis is directed slightly dorsally. The space and bony lamina extending between the dia- and parapophysis are narrower on v8 than on the more anterior vertebrae.

Caudal to the rib-bearers and between the posteri- or interzygapophyseal ridge and the posterior ventral crest a foramen for the spinal nerve is present (Fig. 3D). The foramen is small on the anteriormost vertebrae and becomes very large on the last trunk vertebra (v8).

#### Sacrum

A single sacral vertebra (v9) is present. It is much more robust and depressed than the other vertebrae (Fig. 6A). It is also wider across the rib-bearers than long. The neural arch is clearly depressed, with an angle of 10° between the zygapophyseal plane and the posterior end of the neural arch. The neural spine is reduced to a very weak, almost vestigial ridge. There are three nearly circular subcentral foramina.

The spinal nerve foramen is located on the same position as in the other vertebrae, but is larger than on v8 (Fig. 6B). Two other foramina are present, dorsal and ventral to this spinal nerve foramen; these may represent vascular foramina, and/or roots for the spinal nerve. The dorsalmost foramen is smaller than the ventralmost foramen, and both are much smaller than the spinal nerve foramen. The dorsal foramen is connected to the neural canal, whereas the ventral foramen is connected to one of the subcentral foramina. The ventral foramen was therefore probably a vascular foramen, whereas the dorsal foramen may have been used by an unidentified nerve.

In addition, this vertebra differs from the others by the shape and size of its rib-bearers: they are longer and thicker (Fig. 6A). The diapophysis and parapophysis are in contact with each other on most of their length, but the bony lamina is still present between their distal portions. In dorsal view, the right rib-bearer is longer than the left rib-bearer, because of an outgrowth on the diapophysis. Finally, the sacral vertebra differs from other vertebrae in the absence of a notochordal canal.

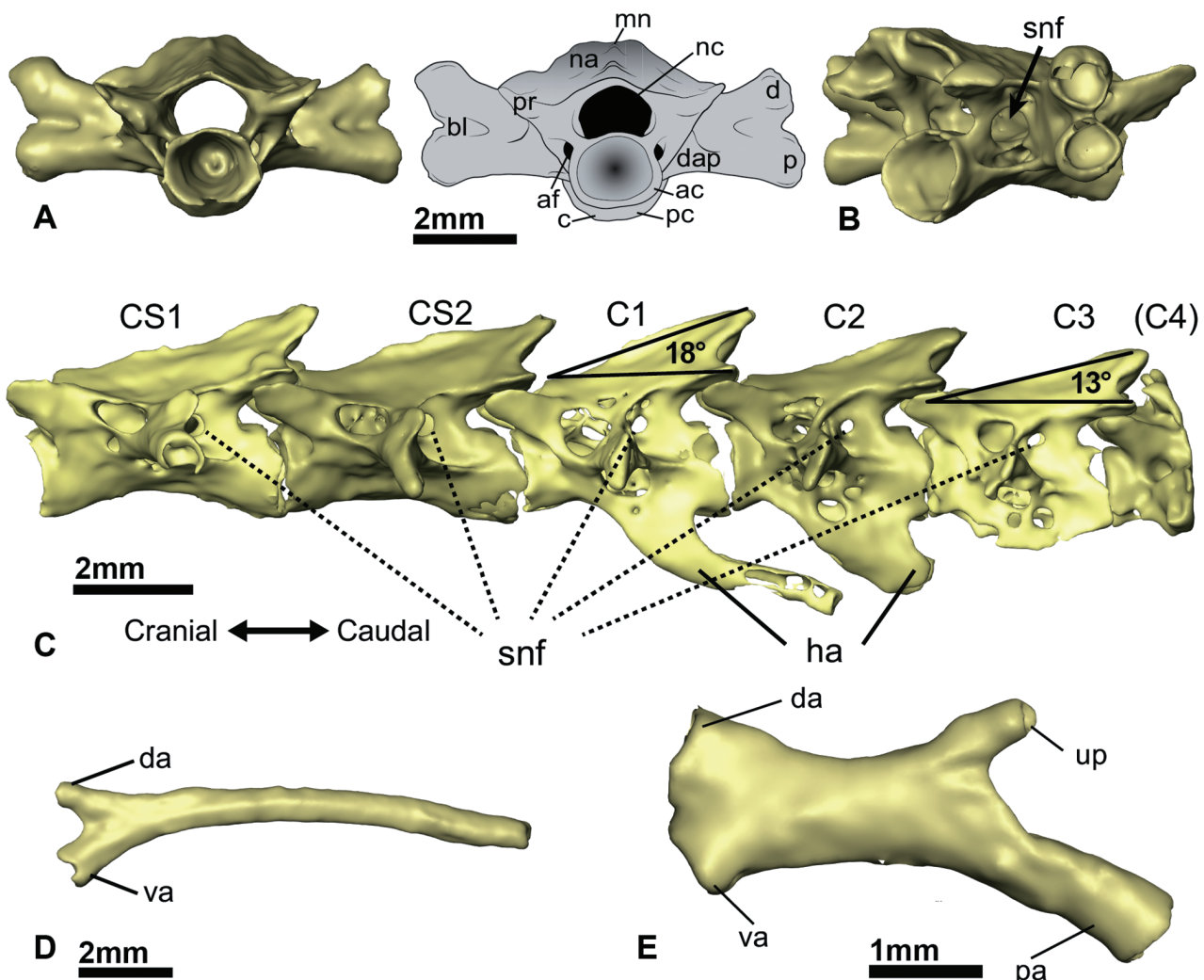


**Figure 6.** A, sacrum in anterior view (left, 3D reconstruction; right, labelled drawing), with abbreviations as defined in the legend to Figure 3. B, sacrum in posterolateral view, illustrating the spinal nerve foramen. C, articulated caudosacral and caudal vertebrae in left lateral view. D, left trunk rib articulating on v3 in anterior view. E, sacral rib in posterior view. Legend: da, dorsal articulation; ha, haemal arch; pa, posteroventral articulation with ilium; up, uncinate process; snf, spinal nerve foramen; va, ventral articulation.

#### Caudal region

At least six postsacral vertebrae are preserved, but the last one (C4) is very incomplete (Fig. 6C). The general morphology of these vertebrae is quite variable. The first two vertebrae (CS1 and CS2) are termed caudosacral: they differ from the more posterior vertebrae, i.e. the caudal vertebrae, in lacking haemal arches (Ratnikov & Litvinchuk, 2007). CS1, CS2, and the first caudal, C1, are wider (rib-bearers included) than long, whereas C2 and C3 are as long as wide. The global size and the width of the neural arch of these vertebrae diminish caudally: CS1 is twice as wide as C3. The neural spine, which is strongly reduced on v8 and on the sacral vertebra, is developed in the caudal

region, except for CS1. The angle between the posterodorsal edge of the neural spine and the zygapophyseal plane varies between 18° (on C1, the highest vertebra) and 13° (on C3), but it does not decrease in a regular way.

Contrary to the other vertebrae, no ribs articulate to the postsacra, even though rib-bearers are still present. On CS1, the diapophysis and parapophysis remain distinct distally, and their extremities still form round facets. On CS2, dia- and parapophysis are still separated distally, but their extremities are compressed anteroposteriorly and they no longer form facets. In the three well-preserved caudals (C1–C3), the dia- and parapophysis merge distally and form a single,

vertically compressed extremity. The size of the rib-bearers decreases posteriorly. The neural spine is thinner and higher than on trunk vertebrae. The spinal nerve foramen of CS1 and CS2 is nearly the same size as on the sacral vertebra; it becomes smaller on the more posterior vertebrae. Other small foramina are present anteroventral and anterodorsal to this foramen, and are irregularly distributed. Several other unidentifiable foramina are present on these vertebrae. The notochordal canal is open.

The haemal arches are at least partly preserved on C1, C2, and C3. They are deeply curved posteriorly (at least on C1, on which it is almost complete; it is too incomplete on the other vertebrae to assess this). The distal extremity does not seem completely ossified.

#### Ribs

Fourteen well-preserved presacral ribs are in anatomical position (eight on the left side and six on the right side), and three others are fragmentary (two on the left side and one on the right side; Fig. 3A). They are all bicapitate, as in most urodeles, and the articular facets are circular. Compared with other urodeles, the ribs are relatively long (Fig. 4), although their length does not reach 10 mm and are weakly curved to almost straight.

#### Presacral ribs

The ventral articular head (which connects to the parapophysis) is usually larger than the head articulating to the diapophysis (Fig. 6D). The diameter of each rib is constant for all of the rib length (the rib does not taper distally; Fig. 3A), except for the articular heads, which are broader. Rib curvature and (even more) length are generally greater cranially than caudally, and the last presacral ribs are nearly straight.

#### Sacral ribs

One sacral rib is connected on each side of the sacral vertebra. They are shorter and more robust than presacral ribs (Fig. 6E). The right one is in anatomical position, whereas the left is slightly disarticulated. The distal extremity of these ribs was connected to the ilia. The three articular facets (for the parapophysis, diapophysis, and ilium) are circular. A short uncinate process is present posterodorsally.

#### Pelvis and femora

The paired ilium and ischium are preserved almost in anatomical position (Fig. 7); the ischium appears to be slightly shifted posteriorly with regard to the ilium. The femur is broken on both sides; only the proximal ends are preserved (Fig. 7A). It is directed anteriorly. The pubis, which ossifies only in some urodele taxa, is not preserved. There is no trace of an epipubis (ypsiloid cartilage).

The ilium comprises two portions (Fig. 7B): the acetabular portion, which articulates ventrally to the femur and the ischium, and a posterodorsally directed shaft, which articulated to the sacral rib. The shaft is straight and it scarcely expands posterodorsally. It lacks crests and its cross section is approximately oval. The median surface of the acetabular region is smooth, as in most urodeles (Roček *et al.*, 2012), and flat. The ventral limit of the ilium is convex; it forms the sutural surface for the pubis and ischium. The anterior area of the sutural surface is broad and semicircular, whereas the posterior part is elongate and clearly narrowed. At least the anterior part of the broad area was in contact with the pubis, whereas the narrow area was sutured to the ischium. The acetabulum is subtriangular and shallowly concave; its anterior margin is parallel with the shaft axis. The articular surface occupies almost the entire acetabular portion. The margins of the acetabulum are not clearly distinct; they do not project laterally, except in their dorsal portion, where they form a marked tubercle. The latter tubercle is not homologous to the ventrolateral tuberosity that occurs in some extant and extinct urodeles (Gardner *et al.*, 2010). The ventrolateral tuberosity is distinct from the acetabular margin, whereas in *P. sigei* gen. et sp. nov. the tubercle is a part of the margin. Ventrally, the articular surface of the acetabulum was completed by the ischium.

The ischium is a thin plate in which the anterior part is only lightly ossified (Fig. 7C). The caudal part produces a short posteromedial process and an elongate, slender posterolateral process. The anterior edge of the ischial plate forms a gutter, which indicates the insertion of the cartilaginous pubis. A medial cartilaginous symphysis probably joined the two plates, but it is not visible on the tomograms. The ventral part of the articular surface of the acetabulum is located anterolaterally on the ischium; it protrudes laterally.

On the femur, the femoral crest (crista trochanterica; Venczel, 2008; Skutschas & Gubin, 2012) is well developed (Fig. 7A). It extends to the greater trochanter, which forms a strong projection directed posteroventrally on the ventral face, close to the proximal extremity of the femur. The outline of the distal extremity of the trochanter is ovoid. The trochanter diverges sharply from the femoral shaft. Between the base of the trochanter and the proximal extremity of the femur, extends the marked trochanteric groove (Vasilyan & Böhme, 2012) that appears to be present in most (all?) urodeles with non-reduced limbs. The cartilaginous cap of the proximal extremity of the femur is not preserved (Fig. 7D).

#### Lung

Several types of soft tissues are preserved and may be identified on the tomograms. A histological study

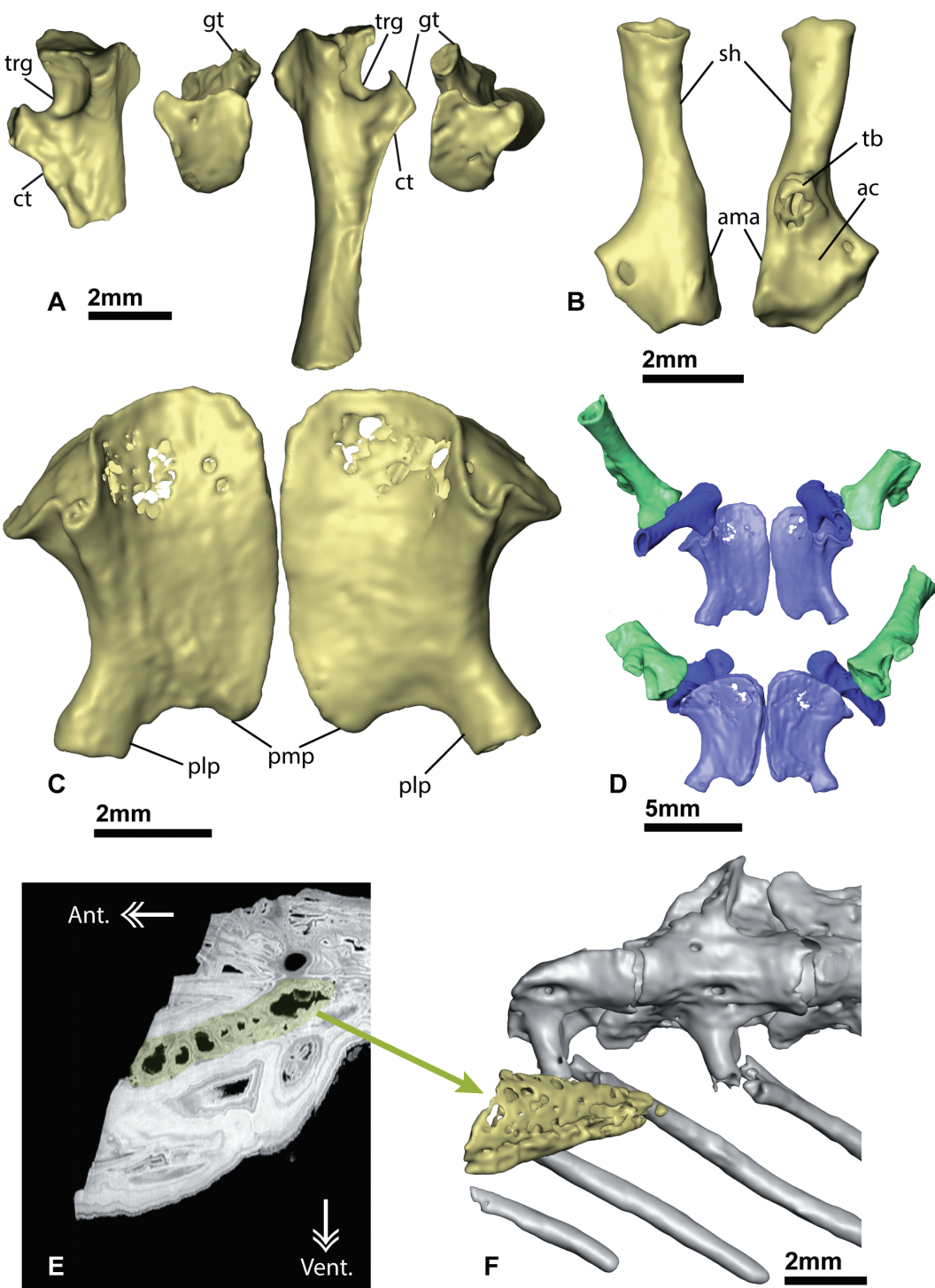


**Figure 7.** Three-dimensional reconstructions of various parts of the skeleton (A–D) and of the lung (E, F). A, right and left femora in lateral and proximal views. B, left ilium in medial and lateral views. C, left and right ischia in dorsal view. D, pelvic bones in dorsal (top) and ventral (bottom) views; green (light grey in print), femur; light blue (medium grey in print), ischium; and dark blue (dark grey in print), ilium. E, virtual cross section of the anteriormost part of MNHN.F.QU17755, showing part of the preserved lung. F, three-dimensional reconstruction of the preserved part of the lung, in ventral view. Abbreviations: ac, acetabulum; ama, anterior margin of the acetabulum; Ant., anterior; ct, crista trochanterica; gt, greater trochanter; plp, posterolateral projection; pmp, posterior median process; sh, shaft; tb, tubercle; trg, trochanteric groove; Vent., ventral.

will be undertaken to determine their nature. One organ is discussed here, however, because it is of significant interest for our phylogenetic study: the lung.

The lung is present at the anteriormost part of the specimen (Fig. 7E). It is triangular in ventral view, with its tip directed caudally, and flattened in cross section (Fig. 7F). The cranial part of the lung is missing, which makes identification difficult. Nevertheless, the position of this organ in the body, its shape, and its ‘honeycombed’ internal structure suggest that it is a lung (Francis, 1984; M. Laurin, pers. observ.).

## PHYLOGENY

One most-parsimonious tree of 3709 steps has been found by the heuristic search. The consistency index (CI) is 0.4627, the homoplasy index (HI) is 0.5384, the retention index (RI) is 0.6543, and the rescaled consistency index (RC) is 0.3027. One tree-island of one tree was found 1000 times. The topology is similar to that obtained by Wiens *et al.* (2005) with the combined data in parsimony, and is identical to the bootstrap tree (Fig. 8). The Sirenidae (*Siren* and *Pseudobranchus*) are now a sister clade to all other Salamandroidea (support value = 62), as in their Bayesian analysis. *Phosphotriton sigei* gen. et sp. nov. is here placed in a stem-salamandrid position.

To determine the relative frequency at which *P. sigei* gen. et sp. nov. is located on various branches of the tree, a complementary bootstrap analysis was performed. Ten sequence-addition replicates were performed for each of the 300 bootstrap search replicates. All trees were saved and the first tree of each of the first 200 bootstrap replicates was observed in a MESQUITE tree window. The placement of *P. sigei* gen. et sp. nov. was then scored for each tree and percentages were calculated [Fig. 8: brown (grey in print) numbers under branches]. *Phosphotriton sigei* gen. et sp. nov. is never placed within the crown Salamandridae or Ambystomatidae, but is frequently found as the sister taxon of the smallest clade that includes the plethodontids *Desmognathus* and *Aneides* (18% of bootstrap trees), or as the sister taxon of either genus, with 5.5 and 3% frequencies, respectively. All in all, *P. sigei* gen. et sp. nov. is found in 44% of the trees within the Plethosalamandroidei (= Plethodontidae + *Rhyacotriton* + *Amphiuma*), which is comparable with the major placement as sister taxon to the Salamandridae (44.5%). It is also sister taxon to *Dicamptodon* in 9% of the bootstrap replicates.

## DISCUSSION

### TAXONOMIC ASSIGNMENT

Character evolution was retraced using parsimony in MESQUITE (Maddison & Maddison, 2014). Four

synapomorphies show that *P. sigei* gen. et sp. nov. belongs to the smallest clade that includes Treptobranchia and Plethosalamandroidea. We use the available name Pseudosauria for this clade. Pseudosauria has been applied to variable concepts by various authors; however, Frost (2014) delimited Pseudosauria approximately as we do here, and we prefer to avoid the erection of a new name. The synapomorphies that argue for assignment to Pseudosauria are the presence of a posterior median process on the ischium (character 206), the absence of articulated ribs on caudal vertebrae (character 237), the separate condition of para- and diapophyses in the trunk region (character 255), and the intravertebral position of the spinal foramen in caudal vertebrae (character 283).

Four synapomorphies whose position is non-ambiguous support the placement of *P. sigei* gen. et sp. nov. in the salamandrid stem. The presence of sacral ribs (character 242) is a synapomorphy of the clade formed by Salamandridae, including *P. sigei* gen. et sp. nov., but it is lost in *Notophthalmus*. A median notch indenting the neural arch of trunk vertebrae (character 254), as well as a ‘low’ neural spine on trunk vertebrae (character 256), which becomes ‘raised’ in *Taricha* and *Notophthalmus*, and the presence of a neural spine on caudal vertebrae (character 260) are synapomorphies of the same clade.

Two other synapomorphies, the positions of which are ambiguous, might support the same placement of *P. sigei* gen. et sp. nov. The first is the presence of a bony lamina between parapophyses and diapophyses (character 243). Because it is also present in *Dicamptodon* (but not in *Ambystoma*), it may be a synapomorphy of Treptobranchia (ACCTRAN optimization) or Salamandridae (DELTRAN optimization). The second possible synapomorphy, for which a similar (although not identical) scheme occurs, is character 282: spinal nerves in posterior trunk vertebrae exiting intravertebrally. Again, this may be a synapomorphy of Treptobranchia (ACCTRAN) or Salamandridae (DELTRAN). It would then have occurred by convergence in *Ambystoma*.

An osteological feature that is not in the character matrix deserves attention: the presence of a dorsal alar process between the parapophysis and the prezygapophysis. As stated above, such a crest occurs only in the Sirenidae and in the Pleurodelini (Salamandridae). As in sirenids, in *P. sigei* gen. et sp. nov. the dorsal alar process is present along with the anterior interzygapophyseal ridge, whereas pleurodelines lack the latter ridge. In sirenids, however, the system of crests and ridges is complex: an additional oblique crest (anterior alar process; Gardner, 2003) originates on the parapophysis, is directed anteroventrally, and appears to be symmetrical to the dorsal alar process. In Pleurodelini, in which the classical, horizontal

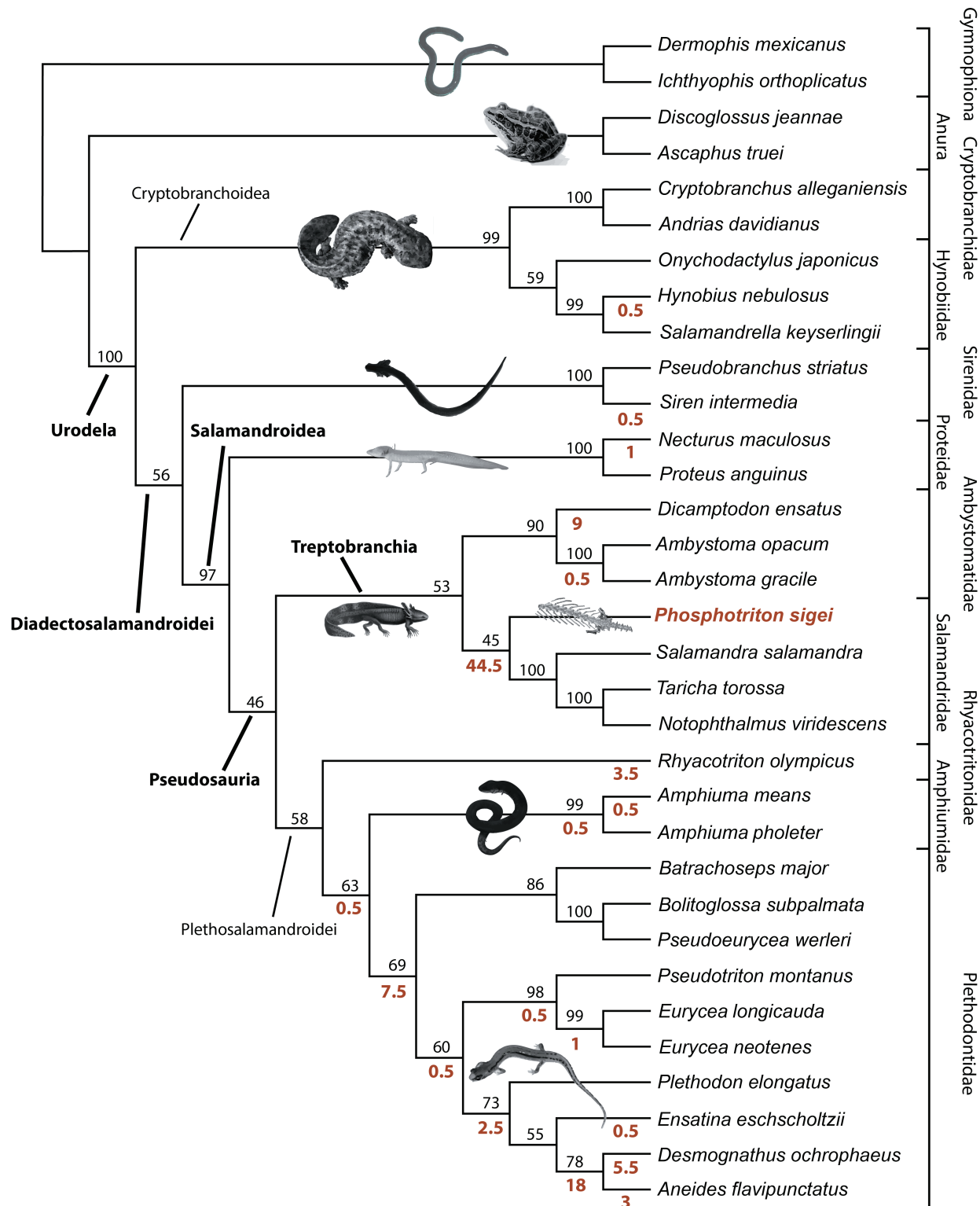


**Figure 8.** Phylogenetic tree of urodeles based on parsimony analysis of morphological and molecular data (modified from the matrix of Wiens *et al.*, 2005), showing the relationships between extant urodeles and ***Phosphotriton sigei* gen. et sp. nov.** Supraspecific names in bold indicate taxa into which the new taxon is included in the majority-rule (50%) consensus tree; numbers above branches, bootstrap values; bold numbers under branches, percentage of trees (among the first tree yielded by each of the 200 bootstrap replicates) in which ***P. sigei* gen. et sp. nov.** is placed on the branch.

anterior interzygapophyseal ridge is absent, the oblique crest (dorsal alar process) was interpreted as the anterior interzygapophyseal ridge, which would have changed its orientation to dive posteroventrally towards the parapophysis (Estes, 1981). The presence of both an anterior interzygapophyseal ridge and a dorsal alar process in the treptobranch *P. sigei* gen. et sp. nov., however, suggests that in pleurodelines, the dorsal alar process may be homologous with that of *P. sigei* gen. et sp. nov., and that the anterior interzygapophyseal ridge is lacking. In any case, the dorsal alar process of *P. sigei* gen. et sp. nov. differs from that of sirenids in lacking the association with an anterior alar process, and from pleurodelines in being associated with an anterior interzygapophyseal ridge. According to the available data, this combination of features of *P. sigei* gen. et sp. nov. appears to be unique; however, we could not examine all extinct and extant urodele taxa.

Even though soft tissues are rarely used in palaeontology for phylogenetic inference, mostly because data are usually lacking, they are not to be ignored. Here, the incorporation of the character ‘lung’ (character 2070) has been very important for the reconstruction of the phylogeny. It was observed during the segmentation process and will be described in a subsequent study, amongst other soft tissues. This character was indeed decisive for the placement of this mummy in the phylogeny. A parsimony analysis was first performed without that character, and in the resulting trees, the specimen was placed in two distinct positions: basal to the Salamandridae and in the Plethodontidae. Therefore, our interpretation of the primitive retention of this organ is decisive for the results presented here. Indeed, the addition of another character (‘vertebral centrum’, character 2069, scored as ‘amphicoelous’ in *P. sigei* gen. et sp. nov.), but a coding of lungs as ‘absent’, had led to a placement of this specimen in the Plethodontidae. The addition of the character ‘lung’ increases the resolution and yields a single most-parsimonious position for *P. sigei* gen. et sp. nov., as sister group of the included extant salamandrids.

Our bootstrap results suggest that approximately the same number of characters coded effectively support the specimen placement presented here as somewhere in Plethosamandroidei. The most frequent placement is that presented on the tree (44.5% of bootstrap replicates), which is the same result as in the heuristic search: as sister group of extant Salamandridae. The second most frequent placement (18% of bootstrap replicates), as sister group of the smallest clade that includes *Desmognathus* and *Aneides* (within Plethodontidae), presumably reflects the fact that a single character (the presence of a lung) precludes this placement, and in several bootstrap replicates this character must be absent. A significant proportion of bootstrap

replicates (39%, which is the sum of all possible significant placements) places *P. sigei* gen. et sp. nov. among a certain number of plethodontid groups (except Bolitoglossinae), which are lungless. Nevertheless, the bootstrap replicates do not appear to give an entirely satisfactory view of the possible affinities of *P. sigei* gen. et sp. nov. The 39% of bootstrap replicates in which *P. sigei* gen. et sp. nov. is located among the lungless plethodontids presumably reflect the fact that in these replicates, the character ‘lung’ had not been sampled. Thus, bootstrapping probably yields overly pessimistic results about the affinities of *P. sigei* gen. et sp. nov., and of fragmentary or headless fossils in general, for which few taxonomic characters can be scored. In this case, the absence of the head is the most severely limiting problem, which is only partly compensated for by the soft-tissue preservation. Future soft-anatomical, histological, and morphometric analyses might lend further support to the position of *P. sigei* gen. et sp. nov. in urodele phylogeny.

Biogeographic considerations also make salamandrid affinities more probable than others because most Eocene and extant salamanders in Europe are salamandrids (Fig. 4D), even though this is a weak criterion. Extant representatives of Ambystomatidae (including dicamptodontines) and Plethosamandroidei (within which *P. sigei* gen. et sp. nov. occurs with low bootstrap frequencies) occur mostly in North America, even though rare plethodontids also occur in southern Europe (Fig. 4A) and eastern Asia; however, strong similarities between Eocene faunas from Europe and North America were noticed (Rage, 2012; Rage & Roček, 2003). Consequently, the presence of a salamander with North American affinities in the Eocene of Europe would not be entirely implausible. Among these taxa with North American affinities, only plethodontids (Fig. 4A) may plausibly be closely related to *P. sigei* gen. et sp. nov.

We consider that the new taxon belongs to Salamandridae, even though we cannot directly determine, given the taxonomic sampling of our data matrix, whether the taxon is part of the salamandrid crown group or not. This is because in our matrix, salamandrids are represented only by *Salamandra*, *Taricha*, and *Notophthalmus*. Yet, according to Pyron & Wiens (2011: fig. 2), the smallest clade that includes these three extant salamandrids is the sister group of *Salamandrina*, which is also a salamandrid. Thus, the new taxon may or may not be part of crown-group salamandrids (although if part of the crown group, it would obviously be located very near its base). We propose to provisionally phylogenetically define Salamandridae, pending implementation of the PhyloCode (Cantino & de Queiroz, 2010), as the largest clade that includes *Salamandra salamandra* (Linnaeus, 1758), but not *Ambystoma opacum* (Gravenhorst, 1807), *Proteus anguinus* (Laurenti, 1768), and *Rhyacotriton*

*olympicus* (Gaige, 1917). This is a branch-based concept, and the use of multiple external specifiers takes into account uncertainties about the identity of the closest relatives of Salamandridae (Wiens *et al.*, 2005; Frost *et al.*, 2006; Pyron & Wiens, 2011). Pending a more definitive assessment of the taxonomic position of the new taxon, and under the phylogenetic definition of Salamandridae proposed here, we consider that *P. sigei* should provisionally be considered a salamandrid. In the context of rank-based nomenclature, we also consider it part of Salamandridae. Furthermore, it should be kept in mind that all extant Salamandridae including *Salamandrina* (Pitruzzella *et al.*, 2008; Venczel & Hír, 2013) are opisthocoelous. With amphicoely being theoretically the plesiomorphic state, the referral of *P. sigei* gen. et sp. nov. to the crown group would imply that opisthocoely developed twice in salamandrids, which is unparsimonious. Therefore, amphicoely supports a stem position for the fossil.

#### GEOLOGICAL AGE

A few facts need to be considered to assess the geological age of the new taxon: bones of *P. sigei* gen. et sp. nov. have not been found among the very numerous fossils collected during the recent excavations, nor in the old collections, which means that this taxon was probably very rare, and prevents any direct dating analysis. However, it seems rather likely that all ‘mummies’ come from a single locality (Filhol, 1877: 24). This is supported by the fact that they were preserved in siderolithic clays (Filhol, 1877: 25), a type of sediment that is not frequent in the phosphorites, and that no other mummy has been discovered in the numerous field trips of the last decades in any Quercy localities. Thus, all mummies are probably of a same geological age, i.e. Late Bartonian (MP16) to Late Priabonian (MP19–20). This age is suggested by the anuran *Thaumastosaurus gezei*, which is known by a mummy and isolated bones from several well-dated localities in the Phosphorites du Quercy (Rage & Roček, 2007; Laloy *et al.*, 2013).

The referral of *P. sigei* gen. et sp. nov. to Treptobranchia is consistent with the previously known stratigraphic range of the group (Marjanović & Laurin, 2014: fig. 2). The earliest known treptobranchs are indeterminate Salamandridae from the Late Cretaceous (Campanian) of France (Sigé *et al.*, 1997; Garcia *et al.*, 2000) and Spain (Duffaud & Rage, 1999). The assignment of the Cretaceous fossils to Salamandridae was at first somewhat uncertain, but was confirmed by Duffaud (2000) and now appears to be reliable. The Ambystomatidae (dicamptodontines included) date back to the late Palaeocene of North America (Naylor & Fox, 1993; Gardner & DeMar, 2013) and also Europe, if the assignment of *Wolterstorffella* and *Geyeriella* to

‘dicamptodontids’ (Estes, 1981) is accurate. Plethosalamandroidea, i.e. the sister group of treptobranchs that includes plethodontids, are first known by amphiumids in the Maastrichtian (perhaps Campanian) of North America (Gardner & DeMar, 2013). Surprisingly, plethodontids have no fossil record earlier than the Early Miocene (Estes, 1981). The phylogenetic position of *P. sigei* gen. et sp. nov. fits well into the palaeontological time tree proposed by Marjanović & Laurin (2014).

#### ACKNOWLEDGEMENTS

We thank the staff of the Centre de Microscopie de fluorescence et d’IMagerie numérique (CeMIM) facilities of the MNHN, and particularly Marc Gèze (MNHN, Paris, France) and Cyril Willig (MNHN, Paris), for letting us use the computers for segmentation of the data and for their help. We thank Yannick Pannier (Pprime Institute, France) for providing access to the tomograph of the Ecole nationale supérieure de mécanique et d’aérotechnique (ENSMA, Chasseneuil-du-Poitou, France). We are grateful to Annemarie Ohler (MNHN, Paris), Anthony Herrel (MNHN, Paris), Salvador Bailon (MNHN, France), as well as Jean-Jacques Jaeger (iPHEP, Poitiers, France) and the Centre de Valorisation des Collections scientifiques de l’Université de Poitiers, France (CVCU), for providing comparison specimens to study. We thank Thierry Pélissié (Phosphatières du Quercy, Bach, France) for information on the history of the ‘Phosphorites du Quercy’ and other topics. James D. Gardner (Royal Tyrrell Museum of Palaeontology, Drumheller, Canada) and Pavel P. Skutschas (Saint Petersburg State University, Russia) provided useful information. J.T., J.-C.R., and M.L. were funded by recurring grants from the CNRS, the French Ministry of Research, and Sorbonne Universités to the CR2P. The synchrotron microtomography experiments were performed on the ID19 (proposal MD727) and ID17 beamline at the European Synchrotron Radiation Facility (ESRF), Grenoble, France. We would like to thank Christian Nemoz and Alberto Bravin for their help and their time. We are very grateful to the two anonymous reviewers who provided constructive remarks on the text.

#### REFERENCES

- Babcock SK, Blais JL. 2001. Caudal vertebral development and morphology in three salamanders with complex life cycles (*Ambystoma jeffersonianum*, *Hemidactylum scutatum*, and *Desmognathus ocoee*). *Journal of Morphology* **247**: 142–159.  
 Bailon S, Rage JC, Stoetzel E. 2011. First fossil representative of the salamander crown-group from a Gondwanan continent: *Pleurodeles cf. walstl* from the Quaternary of Morocco. *Amphibia-Reptilia* **32**: 245–252.

- de Blainville HMD.** 1816. Prodrome d'une nouvelle distribution systématique du règne animal. *Bulletin de la Société philomatique de Paris* **8:** 113–124.
- Cantino PD, de Queiroz K.** 2010. International Code of Phylogenetic Nomenclature. Version 4c. Available at: <http://www.ohio.edu/phylocode/>
- Duffaud S.** 2000. Les faunes d'amphibiens du Crétacé supérieur à l'Oligocène inférieur en Europe: paléobiodiversité, évolution, mise en place. Unpublished Thesis, Muséum national d'Histoire naturelle, Paris.
- Duffaud S, Rage JC.** 1999. Amphibians from the Upper Cretaceous of Laño (Basque Country, Spain). *Estudios del Museo de Ciencias Naturales de Alava* **14** (núm. esp. 1): 111–120.
- Estes R.** 1981. Gymnophiona, Caudata. *Handbuch der Paläoherpetologie*, Vol. 2. Stuttgart: Gustav Fischer Verlag.
- Evans SE, Milner AR, Mussett F.** 1988. The earliest known salamanders (Amphibia, Caudata): a record from the Middle Jurassic of England. *Geobios* **21:** 539–552.
- Filhol H.** 1873. Sur des pièces fossiles provenant de Batraciens, de Lacertiens et d'Ophidiens, trouvées dans les dépôts de phosphates de chaux de l'Aveyron. *Comptes Rendus de l'Académie des Sciences de Paris* **77:** 1556–1557.
- Filhol H.** 1877. *Recherches sur les phosphorites du Quercy*. Paris: Masson.
- Fischer von Waldheim G.** 1813. *Zoognosia tabulis synopticis illustrata, in usum prælectionum Academizæ Imperialis Medico-Chirurgicæ Mosquensis edita*, Vol. 1, 3rd edn. Moscow: Nicolai Sergeidis Vsevolozsky.
- Francis ETB.** 1934. *The anatomy of the salamander*. Oxford: Clarendon Press.
- Frost DR.** 2014. Amphibian Species of the World: an Online Reference. Version 6.0 (accessed February 19, 2015). Available at: <http://research.amnh.org/herpetology/amphibia/index.html> American Museum of Natural History, New York.
- Frost DR, Grant T, Faivovich J, Bain RH, Haas A, Haddad CFB, de Sá RO, Channing A, Wilkinson M, Donnellan SC, Raxworthy CJ, Campbell JA, Blotto B, Moler P, Drewes RC, Nussbaum RA, Lynch JD, Green DM, Wheeler WC.** 2006. The amphibian tree of life. *Bulletin of the American Museum of Natural History* **297:** 1–370.
- Gaige HT.** 1917. Description of a new salamander from Washington. *Occasional papers of the Museum of Zoology, University of Michigan* **40:** 1–3.
- Gao KQ, Shubin NH.** 2001. Late Jurassic salamanders from northern China. *Nature* **410:** 574–577.
- Gao KQ, Shubin NH.** 2012. Late Jurassic salamandroid from western Liaoning, China. *Proceedings of the National Academy of Sciences of the United States of America* **109:** 5767–5772.
- Garcia G, Duffaud S, Feist M, Marandat B, Tambareau Y, Villatte J, Sigé B.** 2000. La Neuve, gisement à plantes, invertébrés et vertébrés du Bégudien (Sénonian supérieur continental) du bassin d'Aix-en-Provence. *Geodiversitas* **22:** 325–348.
- Gardner JD.** 2003. Revision of *Habrosaurus* Gilmore (Caudata, Sirenidae) and relationships among sirenid salamanders. *Paleontology* **46:** 1089–1122.
- Gardner JD, DeMar DG Jr.** 2013. Mesozoic and Palaeocene lissamphibian assemblages of North America: a comprehensive review. In: Gardner JD, Nydam RL, eds. *Mesozoic and Cenozoic lissamphibian and squamate assemblages of Laurasia, Palaeobiodiversity and Palaeoenvironments* **93:** 459–515.
- Gardner JD, Roček Z, Přikryl T, Eaton JG, Blob RW, Sankey JT.** 2010. Comparative morphology of the ilium of anurans and urodeles (Lissamphibia) and a re-assessment of the anuran affinities of *Nezpercius dodsoni* Blob et al., 2001. *Journal of Vertebrate Paleontology* **30:** 1684–1696.
- Goldfuss GA.** 1820. *Handbuch der Zoologie. II*. Nürnberg: Johann Leonhard Schrag.
- Grand A, Corvez A, Duque Velez LM, Laurin M.** 2013. Phylogenetic inference using discrete characters: performance of ordered and unordered parsimony and of three-item statements. *Biological Journal of the Linnean Society* **110:** 914–930.
- Gravenhorst JLCC.** 1807. *Vergleichende Übersicht des Linneischen und einiger neuern zoologischen Systeme*. Göttingen: Heinrich Dietrich.
- Haddoumi H, Allain R, Meslouh S, Métais G, Monbaron M, Pons D, Rage JC, Vullo R, Zouhri S, Gheerbrant E.** 2015. Guelb el Ahmar (Bathonian, Anoual Syncline, eastern Morocco): first continental flora and fauna including mammals from the Middle Jurassic of Africa. *Gondwana Research* doi: 10.1016/j.gr.2014.12.004.
- Hay JM, Ruvinsky I, Hedges SB, Maxson LR.** 1995. Phylogenetic relationships of amphibian families inferred from DNA sequences of mitochondrial 12S and 16S ribosomal RNA genes. *Molecular Biology and Evolution* **12:** 928–937.
- Laloy F, Rage JC, Evans SE, Boistel R, Lenoir N, Laurin M.** 2013. A re-interpretation of the Eocene anuran *Thaumastosaurus* based on microCT examination of a ‘mummified’ specimen. *PLoS ONE* **8:** e74874.
- Larson A, Dimmick WW.** 1993. Phylogenetic relationships of the salamander families: an analysis of congruence among morphological and molecular characters. *Herpetological Monographs* **7:** 77–93.
- Laurenti JN.** 1768. Specimen medicum, exhibens synopsin reptilium emendatam cum experimentis circa venena et antidota reptilium Austriacorum. PhD thesis, Vienna.
- Legendre S, Sigé B, Astruc JG, de Bonis L, Crochet J-Y, Denys C, Godinot M, Hartenberger J-L, Lévéque F, Marandat B, Mourer-Chauviré C, Rage JC, Remy JA, Sudre J, Vianey-Liaud M.** 1997. Les phosphorites du Quercy: 30 ans de recherche. Bilan et perspective. *Geobios, mémoire spécial* **20:** 331–345.
- Linnaeus C.** 1758. *Systema naturae*. Stockholm: Laurentii Salvii.
- Maddison WP, Maddison DR.** 2014. Mesquite: a modular system for evolutionary analysis. Version 3. Available at: <http://mesquiteproject.org>
- Marjanović D, Laurin M.** 2007. Fossils, molecules, divergence times, and the origin of lissamphibians. *Systematic Biology* **56:** 369–388.
- Marjanović D, Laurin M.** 2014. An updated paleontological timetree of lissamphibians, with comments on the anatomy of Jurassic crown-group salamanders (Urodela). *Historical Biology* **26:** 535–550.

- Mirone A, Brun E, Gouillart E, Tafforeau P, Kieffer J.** 2014. The PyHST2 hybrid distributed code for high speed tomographic reconstruction with iterative reconstruction and a priori knowledge capabilities. *Nuclear Instruments and Methods in Physics Research Section B: Beam Interactions with Materials and Atoms* **324**: 41–48.
- Naylor BG, Fox RC.** 1993. A new ambystomatid salamander *Dicamptodon antiquus* n. sp., from the Paleocene of Alberta, Canada. *Canadian Journal of Earth Sciences* **30**: 814–818.
- Paganin D, Mayo S, Gureyev TE, Miller PR, Wilkins SW.** 2002. Simultaneous phase and amplitude extraction from a single defocused image of a homogeneous object. *Journal of Microscopy* **206**: 33–40.
- Pitruzzella G, Delfino M, Böhme M, Rook L.** 2008. Osteology of genus *Salamandrina*: preliminary observation from a paleontological perspective. In: Corti C, ed. *Herpetologia Sardiniae*. Societas Herpetologica Italica/Edizioni Belvedere, Latina, le scienze **8**: 412–415.
- Pyron RA.** 2011. Divergence-time estimation using fossils as terminal taxa and the origins of Lissamphibia. *Systematic Biology* **60**: 466–481.
- Pyron RA, Wiens JJ.** 2011. A large-scale phylogeny of Amphibia including over 2800 species, and a revised classification of extant frogs, salamanders, and caecilians. *Molecular Phylogenetics and Evolution* **61**: 543–583.
- Rage JC.** 2006. The lower vertebrates from the Eocene and Oligocene of the phosphorites du Quercy (France): an overview. In: Pélissié T, Sigé B, eds. 30 millions d'années de biodiversité dynamique dans le paléokarst du Quercy. *Strata* **13**: 161–173.
- Rage JC.** 2012. Amphibians and squamates in the Eocene of Europe: what do they tell us? In: Lehmann T, Schaal SFK, eds. Messel and the terrestrial Eocene. *Palaeobiodiversity and Palaeoenvironments* **92**: 445–457.
- Rage JC, Roček Z.** 2003. Evolution of anuran assemblages in the Tertiary and Quaternary of Europe, in the context of palaeoclimate and palaeogeography. *Amphibia-Reptilia* **24**: 133–167.
- Rage JC, Roček Z.** 2007. A new species of *Thaumastosaurus* (Amphibia: Anura) from the Eocene of Europe. *Journal of Vertebrate Paleontology* **27**: 329–336.
- Ratnikov VY, Litvinchuk SN.** 2007. Comparative morphology of trunk and sacral vertebrae of tailed amphibians from Russia and adjacent countries. *Russian journal of Herpetology* **14**: 177–190.
- Rineau V, Grand A, Zaragueta R, Laurin M.** 2015. Experimental systematics: sensitivity of cladistic methods to polarization and character ordering schemes. *Contributions to Zoology* **84**: 129–148.
- de Rochebrune AT.** 1884. Faune ophiologique des Phosphorites du Quercy. *Mémoires de la Société des Sciences naturelles de Saône-et-Loire* **5**: 149–164.
- Roček Z, Gardner JD, Eaton JG, Přikryl T.** 2012. Similarities and differences in the ilia of Late Cretaceous anurans and urodeles. *Bulletin de la Société géologique de France* **183**: 529–535.
- Sanchiz B.** 1998. Salientia. In: Wellnhofer P, ed. *Encyclopedia of Paleoherpetology*. Munich: Dr. Friedrich Pfeil. 1–275.
- Sigé B, Aguilar J-P, Marandat B, Astruc J-G.** 1991. Extension au Miocène inférieur des remplissages phosphatés du Quercy. La faune de vertébrés de Crémat (Lot, France). *Geobios* **24**: 497–502.
- Sigé B, Buscalioni AD, Duffaud S, Gayet M, Orth B, Rage JC, Sanz JL.** 1997. Etat des données sur le gisement crétacé supérieur continental de Champ-Garimond (Gard, sud de la France). *Münchner Geowissenschaftliche Abhandlungen A* **34**: 111–130.
- Sigé B, Pélissié T.** 2006. Avant-propos. In: Pélissié T, Sigé B, eds. 30 millions d'années de biodiversité dynamique dans le paléokarst du Quercy. *Strata* **13**: 5–7.
- Skutschas PP.** 2013. Mesozoic salamanders and albanerpetontids of Middle Asia, Kazakhstan, and Siberia. *Palaeobiodiversity and Palaeoenvironments* **93**: 441–457.
- Skutschas PP, Baleeva NV.** 2012. The spinal cord supports of vertebrae in the crown-group salamanders (Caudata, Urodea). *Journal of Morphology* **273**: 1031–1041.
- Skutschas PP, Gubin YM.** 2012. A new salamander from the late Paleocene–early Eocene of Ukraine. *Acta Palaeontologica Polonica* **57**: 135–148.
- Skutschas PP, Martin T.** 2011. Cranial anatomy of the stem salamander *Kokartus honorarius* (Amphibia: Caudata) from the Middle Jurassic of Kyrgyzstan. *Zoological Journal of the Linnean Society* **161**: 816–838.
- Swofford DL.** 2003. PAUP\* Phylogenetic Analysis Using Parsimony (\*and other methods). Version 4.0b10 ed. Sunderland, Massachusetts: Sinauer Associates.
- Vasilyan D, Böhme M.** 2012. Pronounced peramorphosis in lissamphibians – *Aviturus exsecratus* (Urodea, Cryptobranchidae) from the Paleocene-Eocene Thermal Maximum of Mongolia. *PLoS ONE* **7**: e40665.
- Venczel M.** 2008. A new salamandrid amphibian from the Middle Miocene of Hungary and its phylogenetic relationships. *Journal of Systematic Palaeontology* **6**: 41–59.
- Venczel M, Hír J.** 2013. Amphibians and squamates from the Miocene of Felsőtárkány Basin. *Palaeontographica A* **300**: 117–158.
- Wake DB, Lawson R.** 1973. Developmental and adult morphology of the vertebral column in the plethodontid salamander *Eurycea bislineata*, with comments on vertebral evolution in the Amphibia. *Journal of Morphology* **139**: 251–300.
- Wang Y, Evans SE.** 2006. A new short-bodied salamander from the Upper Jurassic/Lower Cretaceous of China. *Acta Palaeontologica Polonica* **51**: 127–130.
- Wiens JJ.** 2007. Global patterns of diversification and species richness in amphibians. *The American Naturalist* **170**: S86–S106.
- Wiens JJ, Bonett RM, Chippindale PT.** 2005. Ontogeny discombobulates phylogeny: paedomorphosis and higher-level salamander relationships. *Systematic Biology* **54**: 91–110.

**Zhang G, Wang Y, Jones MEH, Evans SE.** 2009. A new early cretaceous salamander (*Regalerpeton weichangensis* gen. et sp. nov.) from the Huaiyiying Formation of northeastern China. *Cretaceous Research* **30**: 551–558.

**Zhang P, Wake DB.** 2009. Higher-level salamander relationships and divergence dates inferred from complete mitochondrial genomes. *Molecular Phylogenetics and Evolution* **53**: 492–508.

#### SUPPORTING INFORMATION

Additional supporting information may be found in the online version of this article at the publisher's web-site:

**Table S1.** Table of tomography parameters.

**Appendix S1.** Data matrix in MESQUITE Nexus format and the most-parsimonious tree.